High-Power BAW-Based FDD Front-End using Indirect-Duplexing Load Modulated Balanced Amplifier for Massive MIMO Array

Yuchen Cao, Shakthi Priya Gowri, Niteesh Bharadwaj Vangipurapu and Kenle Chen Qorvo Inc., INSPIRE Lab, University of Central Florida

yuchen.cao@gorvo.com, contactshakthipriya@gmail.com, ni761834@ucf.edu, kenle.chen@ucf.edu

Abstract — This paper reports a novel high-power frequencydivision duplex (FDD) front-end based on indirect-duplexing load modulated balanced amplifier (LMBA) with integrated bulk acoustic wave (BAW) filters, strongly facilitating the integration into emerging array-based systems. By transforming the BAW device from the antenna interface to the output of control amplifier (CA) together with the intrinsic signal-routing capability of quadrature coupler, the functionality of simultaneous transmission and reception (STAR) is maintained from the standard cavity-based high-power duplexing front-end. More importantly, the size, weight, and cost of the proposed solution are minimized. A commercial BAW Band1/3 quadplexer is integrated with a GaN-based pseudo-Doherty LMBA, achieving $\approx 60\%$ and $\approx 43\%$ of PA efficiency at peak power and 10-dB power back-off, respectively, and low reception loss close to the standalone quadplexer response in modulated measurement.

Keywords — Balanced amplifier, Doherty, frequency-division duplex, high efficiency, high-PAPR, load modulation, multi-band, power amplifier, quadplexer.

I. INTRODUCTION

The powerful next-G network features elevated data rate, minimal latency, and expanded capacity, which necessitates complex modulations, such as OFDM, causing high amplitude fluctuations quantified as peak-to-average power ratio (PAPR). Load modulation is an effective technology for efficient transmission of high-PAPR signals, and its typical implementation, Doherty power amplifier (DPA), has been widely adopted in base stations [1], [2]. However, towards the next-G applications, traditional DPAs face several challenges, including 1) insufficient output power back-off (OBO) range for >10-dB PAPR of 5G/6G signals, 2) inherently narrow bandwidth due to the $\lambda/4$ lines in its generic circuitry. The recently proposed load modulation balanced amplifier (LMBA) [3] is promising to extend both the bandwidth and OBO range with many successful demonstrations [4], [5], [6], [7], [8], [9].

On the other hand, the wireless system has been evolving from single-antenna to many-antenna, also known as massive MIMO. With large antenna array and digital beamforming, mMIMO can significantly enhance the spectrum efficiency through spatial diversity. Nevertheless, each antenna element is associated with a dedicated radio front-end that must be light-weight, compact, and highly efficient to facilitate the array integration. Particularly, the integration of high-Q filters has been recognized as a major bottleneck. While substantial progress has been made by transforming air cavity to dielectric cavity [10], [11], a further miniaturization of filter is still necessary especially for multi-band/carrier-aggregation FDD systems that requires multiple filters.

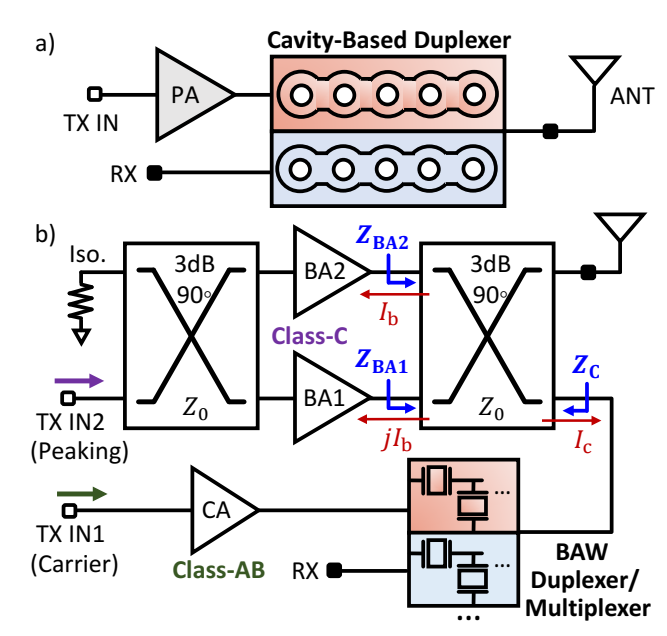


Fig. 1. Conceptual overview and comparison: a) conventional high-power FDD front-end with cavity-based duplexer, b) proposed indirect-duplexing LMBA with integrated BAW device and equivalent FDD functionality.

To facilitate the massive-array integration of high-Q filters, this paper proposes to enable BAW duplexers in high-power FDD front-end by indirectly incorporating the duplexing function into LMBA, as illustrated in Fig. 1. Placed between CA and the isolation port of output quadrature coupler, the BAW duplexer only handles the CA power ($\approx P_{\rm Out,Max.}/10$) in PD-LMBA [5]). Similar to the BA-based STAR front-end [12], [13], the FDD operation is sustained at the antenna interface by leveraging the high $\Gamma_{\rm out}$ (S₂₂) of two BAs in LMBA. Meanwhile, the efficiency enhancement of LMBA can be maintained by adding extra phase delay at the BA path, which can be easily realized with a dual-input design. More importantly, this architecture can be expanded to multi-band design together with BAW multiplexer. To proof the concept, a physical prototype is designed and implemented using GaN-based LMBA and commercial BAW multiplexer, demonstrating efficient transmission and low-loss reception experimentally at 4G-LTE/5G-NR FDD Band 1 and 3.

II. INDIRECT-DUPLEXING LMBA AS FDD FRONT-END

The PD-LMBA with indirect BAW duplexing shown in Fig. 1 can enable concurrent transmission (TX) and reception (RX) at designated frequencies, which are theoretically analyzed in the two subsections below.

A. Transmission with Pseudo-Doherty LMBA

The TX path of proposed FDD front-end needs to be configured as PD-LMBA [5], where the balanced amplifier in PD-LMBA is biased in Class-C as the 'peaking branch' and CA in Class-AB or Class-F/F⁻¹ as the 'carrier branch', as depicted in Fig. 1. In theory, the load modulation of CA and BA in PD-LMBA can be described as

$$Z_{\rm BA1} = Z_{\rm BA2} = Z_0 (1 + \frac{\sqrt{2} I_c e^{j\theta}}{I_b}),$$
 (1)

$$Z_{\rm CA} = Z_0, \tag{2}$$

where I_b is the magnitude of BA currents, I_c is the magnitude of CA current, and θ is the phase offset. The insertion of an extra TX filter between CA and coupler clearly changes the circuit setting, and its impact is analyzed and compensated for in two regions for sustaining the PD-LMBA operation.

- Low-Power Region ($P_{\rm Out} < P_{\rm Max}/{\rm OBO}$): In this region, the BAs are not turned on, $I_b=0$, and the output power is completely generated by the CA, so that the overall LMBA efficiency is equal to the CA efficiency. It should be noted that the added 50- Ω filter not affect CA since it is not load modulated. When the input power reaches the target OBO power, CA is designed to reach saturation for maximum back-off efficiency.
- High-Power Region $(P_{\text{Max}}/\text{OBO} \leq P_{\text{Out}} \leq P_{\text{Max}})$: As the power increases to the target OBO power, the BA is turned on and I_b starts to increase. As an additional phase of ψ from the filter is added between BA and CA, the same phase ψ needs to be offset at the BA input so that the original condition of θ as well as the load modulation of BA can be maintained, as shown in Fig. 2(a), BA and CA maintain the same phase difference θ where connected to the coupler.

B. Low-Loss Reception

The BA has been recently revealed to enable STAR operation [12], [13]. As illustrated in the (Fig. 1), a low-power RX signal received from antenna is quadrature split and impressed upon the output of the two sub-PAs of the balanced topology. It is crucial that the impressed RX signal is strongly and identically reflected by the respective outputs of the BA sub-amplifiers, due to the orthogonality between TX and RX. Subsequently, these reflected RX signals get quadrature combined at the isolated port of BA. Therefore, the BAs' large-signal output reflection coefficient, $|\Gamma_{\rm out}|$, should be maximized to lower the RX path loss. As the expression of $|\Gamma_{\rm out}|$ given in Fig. 2, the design should be conducted towards maximizing the mismatch between the PA static loadline ($Z_{\rm PA}$) (provided collectively by parasitics and OMN) and the reverse impedance looking backwards to the device drain node ($Z_{\rm R}$).

C. Design Space Analysis

In standard BA-based STAR front-end, the two sub-PAs see an identical static load of Z_0 at the coupler plane, which also determines their $|\Gamma_{\rm out}|$. In indirect-duplexing LMBA, the load of BA1 and BA2 are modulated by the LMBA factor

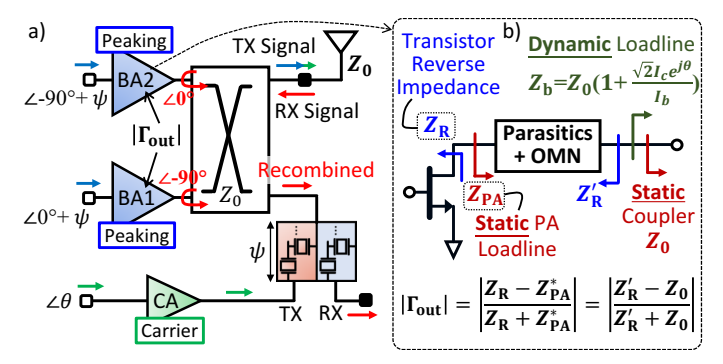


Fig. 2. Operational principle of the indirect-duplexing LMBA with STAR capability enabled by highly reflective loadline design of BA: a) orthogonal TX and RX signal paths, b) formulation of load modulation (TX) and BA1/2 output reflection coefficient (RX).

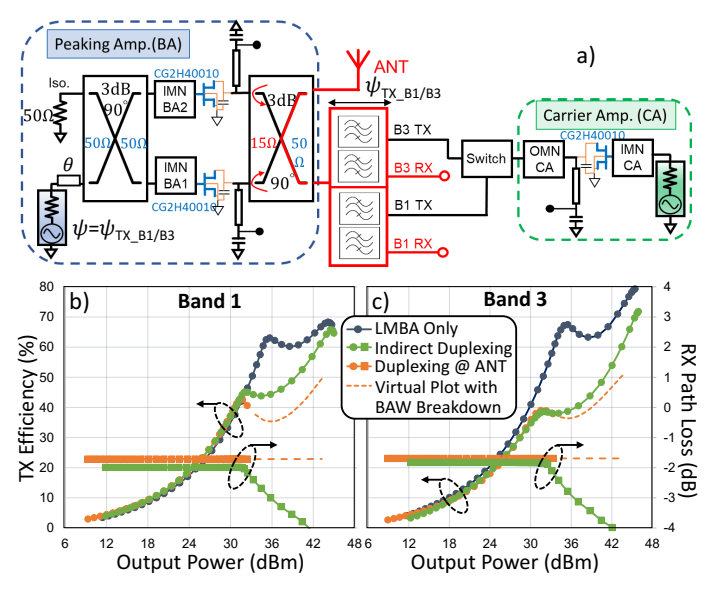


Fig. 3. (a) Circuit schematic of realistically prototyped indirect-duplexing LMBA using GaN devices and commercial BAW multiplexer; (b)-(c) Simulation results of TX efficiency and RX loss at Band 1 and 3.

 $Z_0(1+\sqrt{2}I_ce^{j\theta}/I_b)$, which is seen from the TX perspective. However, examining the same circuit from the RX angle, $|\Gamma_{\rm out}|$ of BA1 and BA2 are still solely dependent on the static load of Z_0 , as indicated in Fig. 2. It is important to note that the difference of BA's load between TX and RX operations offers extended design space. As a result, we can properly design the BA output matching network to achieve optimized load modulation behavior together with a maximized $|\Gamma_{\rm out}|$, in order to optimize the overall TX efficiency and RX loss.

III. PRACTICAL DESIGN OF INDIRECT-DUPLEXING LMBA

Based on the design theory in Sec. II and the ideal schematic in Fig. 1, the physical circuits of CA and BA in the indirect duplexing PD-LMBA are built using 10-W GaN transistors (Wolfspeed CG2H40010F). The selected duplexer is Band 1/3/7 Multiplexer (Qorvo QM26001). The realized circuit schematic is shown in Fig. 3(a). In order to accommodate the high PAPR of emerging 5G and Wifi6 signals, the target OBO of PD-LMBA is designated to 10 dB. The target operation frequency range is to cover Band 1 and Band 3 due to the limited routing capability of single-layer

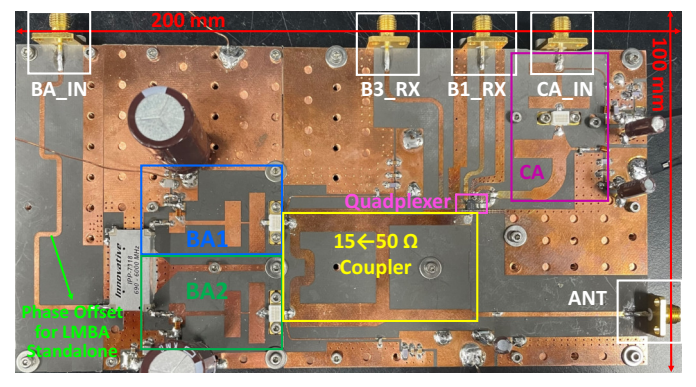


Fig. 4. Fabricated indirect-duplexing PD-LMBA prototype for Band 1 and 3.

PCB. The switching between two bands can be realized using an SP2T RF switch realistically, and it is conducted manually in this proof-of-concept demonstration.

A. Co-Design of BA and CA for High η_{TX} and Low RX Loss

The saturation efficiency of CA determines the back-off efficiency of PD-LMBA. Therefore, in order to maximize the back-off efficiency, a simplified harmonic control output matching network (OMN) similar to [6] is designed to realize the CA continuous mode for wideband operation, as shown in Fig. 4. The peak efficiency of the entire PA is mainly determined by BA. The output coupler is realized with a $15-\Omega$ to $50-\Omega$ two-stage branch-line hybrid coupler, which together with the bias line as a shunt inductor, can provide a desired loadline to BA1 and BA2 over the target bandwidth [14]. The selection of 15- Ω impedance is an optimal trade-off between 1) high peak power and efficiency, and 2) high $|\Gamma_{\rm out}|$ of BA and low RX loss, as illustrated in Fig. 2. A multi-section transmission line matching network is used as input matching for BA and CA to cover the target bandwidth [15]. The BA input coupler is constructed using commercial equipment (IPP-7118, Innovative Power Product [16]) with a wide operating bandwidth of 1.7 to 3.0 GHz.

B. Co-Design of BA-CA Phase Shifter with B1/B3 Duplexer

For standalone PD-LMBA design, a long phase-shifting line is needed at BA input to provide proper BA-CA phase offset [5], [8], which is implemented on the same PCB of indirect-duplexing LMBA, as shown in Fig. 4. When the TX filter of duplexer is inserted between the CA and coupler, a large extra phase shifting of ψ is introduced in the CA path. This is compensated for by adding an external delay at the BA input port, which is adjusted for switching between Band 1 and Band 3.

C. Simulation Results

The simulation results of Band 1 and 3 are shown in Figs. 3(b)-(c). For TX performance, the overall efficiency exhibits a clear enhancement at power back-off just like the standalone LMBA. The degradation of the first efficiency peak is mainly due to the loss of TX filter. Nevertheless, a higher average efficiency is observed compared to LMBA with direct duplexing at the antenna interface, due to the fact that

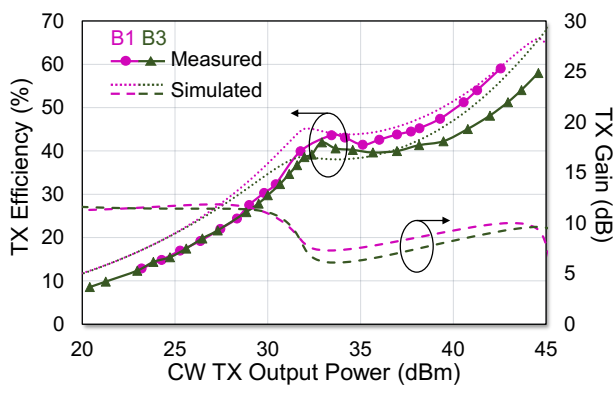


Fig. 5. Measured over TX efficiency versus output power in continuous-wave (CW) measurement.

the power generated by peak amplifier is not subject to the filter loss. The RX loss of Band 1 and 3 is also plotted in Fig. 3(b)-(c). It can be seen that the high $\Gamma_{\rm out}$ of BA leads to a small extra loss of <2 dB added to RX path in high-power region. Given the fact that the average power with modulated TX signal is much lower than the peak, the average RX loss is expected to be close to the original duplexer loss.

IV. IMPLEMENTATION AND EXPERIMENTAL RESULTS

The PD-LMBA with the duplexer connected at the CA port is implemented on a 20-mil thick Rogers Duroid-5880 PCB board with a dielectric constant of 2.2. The fabricated PA mounted on a copper substrate for handling and measurement, is shown in Fig. 4. The CA is biased in Class-F/F $^{-1}$ with a $V_{\rm DS,CA}$ around 10 V. Both the BAs are biased in Class-C with a drain bias of 28-V $V_{\rm DS,BA}$. This prototype is measured with both continuous-wave (CW) and modulated stimulus signals. In this design, the operation is manually switched between Band 1 and 3 frequencies as a proof of concept, where a high value SMD capacitor is used to provide RF short for the band required, whereas the SMD pads of the other path are unconnected.

A. Continuous-Wave Measurement

For the continuous-wave measurement, we can leverage dual input functionality of this PD-LMBA with indirect duplexer design. The two inputs for BA and CA are obtained through splitting from a single CW stimulus. In this testing, an external coaxial cable equal to phase delay of the duplexer is added to the BA path, which can be easily provided and optimized by the CW source for optimum performance. The transmission performance is evaluated at the center frequency of both TX bands, i.e. 1.95 GHz for Band-1 TX and 1.748 GHz for Band-3 TX at different power levels. Fig. 5 shows the TX efficiency of both Band 1 and 3 plotted versus the output power. The measured Band-1 TX efficiency is 60% at the peak output power of 43 dBm, together with the 10-dB back-off efficiency at 42%. In case of Band-3 TX, the peak output power is 44 dBm with a corresponding efficiency of 58%, whilst the 10-dB back-off efficiency is 41%. A strong efficiency enhancement behavior can be observed, throughout the back-off region.

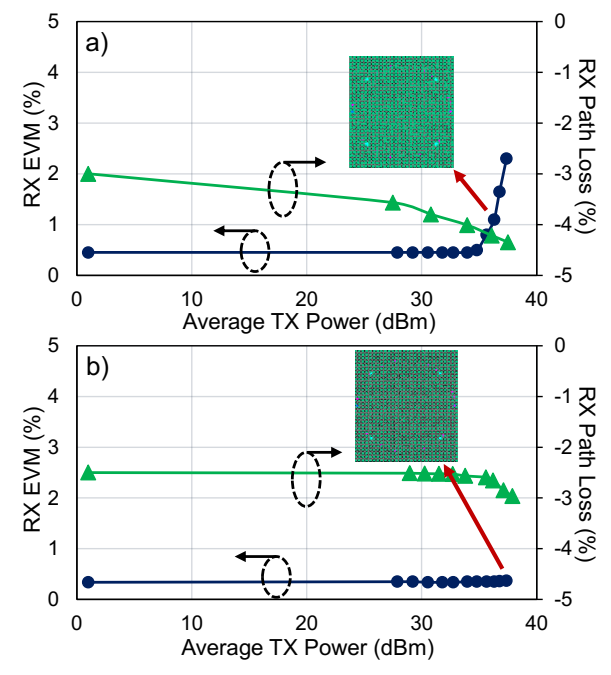


Fig. 6. Measured RX EVM (1024QAM 20-MHz LTE FDD signal) and path loss under modulated TX (256QAM 10-MHz LTE FDD signal) excitation with swept average power: a) Band 1, b) Band 3.

B. Modulated Measurements

In order to evaluate the linearity performance of the RX path, a 20-MHz-bandwidth 1024QAM LTE signal is applied at the input of the receiver path for one band at a time. The TX is also stimulated with a modulated LTE signal (10-MHz bandwidth, 256QAM, 10-dB PAPR) concurrently at both BA and CA inputs. The modulated signals are generated and analyzed with Keysight PXIe vector transceiver (VXT M9421). As shown in Fig. 6, very low EVM < 2.5% and < 0.5% are measured for Band 1 and 3, respectively, indicating highly linear RX paths under the average TX power of up to 37 dBm. Furthermore, the added loss of RX is < 0.9-dB for Band 1 and < 0.5-dB for Band 3.

V. CONCLUSION

An innovative high-power FDD front-end that utilizes an indirect-duplexing LMBA with integrated BAW filters is proposed for the first time in this paper. The design is optimized for seamless integration into emerging array-based systems. Key modifications include relocating the BAW device and leveraging the signal-routing capabilities of a quadrature coupler. This preserves STAR functionality from standard cavity-based systems while minimizing the solution's size, weight, and cost. The integration features a commercial BAW Band 1/3 quadplexer with a GaN-based PD-LMBA, achieving notable PA efficiency and low reception loss. Specifically, the system attains approximately 60% and 43% PA efficiency at peak power and 10-dB power back-off, respectively. Additionally, the harmonics of the large TX signal from BA could be suppressed by adding a lowpass network at output. Overall, this design demonstrates promising performance and cost-effectiveness in integrated array-based systems.

REFERENCES

- [1] V. Camarchia, M. Pirola, R. Quaglia, S. Jee, Y. Cho, and B. Kim, "The Doherty power amplifier: Review of recent solutions and trends," *IEEE Transactions on Microwave Theory and Techniques*, vol. 63, no. 2, pp. 559–571, 2015.
- [2] H. Lyu, Y. Cao, and K. Chen, "Linearity-enhanced quasi-balanced Doherty power amplifier with mismatch resilience through series/parallel reconfiguration for Massive MIMO," *IEEE Transactions on Microwave Theory and Techniques*, vol. 69, no. 4, pp. 2319–2335, 2021.
 [3] D. J. Shepphard, J. Powell, and S. C. Cripps, "An efficient broadband
- [3] D. J. Shepphard, J. Powell, and S. C. Cripps, "An efficient broadband reconfigurable power amplifier using active load modulation," *IEEE Microwave and Wireless Components Letters*, vol. 26, no. 6, pp. 443–445, June 2016.
- [4] T. Cappello, P. H. Pednekar, C. Florian, Z. Popovic, and T. W. Barton, "Supply modulation of a broadband load modulated balanced amplifier," in 2018 IEEE/MTT-S International Microwave Symposium - IMS, June 2018, pp. 304–307.
- [5] Y. Cao and K. Chen, "Pseudo-Doherty load-modulated balanced amplifier with wide bandwidth and extended power back-off range," *IEEE Trans. Microw. Theory Techn.*, vol. 68, no. 7, pp. 3172–3183, 2020
- [6] Y. Cao, H. Lyu, and K. Chen, "Continuous-mode hybrid asymmetrical load-modulated balanced amplifier with three-way modulation and multi-band reconfigurability," *IEEE Transactions on Circuits and Systems I: Regular Papers*, vol. 69, no. 3, pp. 1077–1090, 2022.
- [7] P. Saad and R. Hou, "Symmetrical load modulated balanced power amplifier with asymmetrical output coupling for load modulation continuum," *IEEE Transactions on Microwave Theory and Techniques*, vol. 70, no. 4, pp. 2315–2327, 2022.
- [8] Y. Cao, H. Lyu, and K. Chen, "Asymmetrical load modulated balanced amplifier with continuum of modulation ratio and dual-octave bandwidth," *IEEE Trans. Microw. Theory Techn.*, vol. 69, no. 1, pp. 682–696, 2021.
- [9] J. Pang, Y. Li, M. Li, Y. Zhang, X. Y. Zhou, Z. Dai, and A. Zhu, "Analysis and design of highly efficient wideband RF-input sequential load modulated balanced power amplifier," *IEEE Trans. Microw. Theory Techn.*, vol. 68, no. 5, pp. 1741–1753, 2020.
- [10] R. Mansour, "Filter technologies for wireless base stations," *IEEE Microwave Magazine*, vol. 5, no. 1, pp. 68–74, 2004.
- [11] X. Y. Zhang and J.-X. Xu, "Multifunctional filtering circuits: 3d multifunctional filtering circuits based on high-Q dielectric resonators and coaxial resonators," *IEEE Microwave Magazine*, vol. 21, no. 3, pp. 50–68, 2020.
- [12] D. Regev, S. Shilo, D. Ezri, and G. Ming, "Modified re-configurable quadrature balanced power amplifiers for half and full duplex rf front ends," in 2018 Texas Symposium on Wireless and Microwave Circuits and Systems (WMCS), 2018, pp. 1–4.
- [13] N. B. Vangipurapu and K. Chen, "Magnetic-less simultaneous transmit and receive front end using highly efficient gan-based quadrature balanced amplifier," in 2023 IEEE Wireless and Microwave Technology Conference (WAMICON), 2023, pp. 101–104.
- [14] M. Muraguchi, T. Yukitake, and Y. Naito, "Optimum design of 3-db branch-line couplers using microstrip lines," *IEEE Transactions on Microwave Theory and Techniques*, vol. 31, no. 8, pp. 674–678, Aug 1983.
- [15] K. Chen and D. Peroulis, "Design of highly efficient broadband class-E power amplifier using synthesized low-pass matching networks," *IEEE Transactions on Microwave Theory and Techniques*, vol. 59, no. 12, pp. 3162–3173, Dec 2011.
- [16] Innovative Power Products, NY, USA. 90 Degree Hybrid Couplers. (2015). Accessed: Sep. 15, 2019. [Online]. Available: https://innovativepp.com/product/ipp-7109/.